

1 **HyDRA: a pipeline for integrating long- and short-read RNAseq data for custom**
2 **transcriptome assembly**

3

4 Isabel Almeida^{1,2}, Xue Lu¹, Stacey L. Edwards^{1,2,3}, Juliet D. French^{1,2,3,4}, Mainá Bitar^{1,2,3,4*}

5

6 ¹ Cancer Program, QIMR Berghofer Medical Research Institute, Brisbane, 4029, Australia.

7 ² Faculty of Medicine, The University of Queensland, Brisbane, 4006, Australia.

8 ³ Faculty of Health, Queensland University of Technology, Brisbane, 4006, Australia.

9 ⁴ These authors contributed equally.

10

11 *Correspondence:

12 Mainá Bitar, QIMR Berghofer Medical Research Institute, 300 Herston Road, Herston, Australia

13 4006. Phone: +61 7 38453070. Email: Maina.Bitar@qimrberghofer.edu.au

14

15

16

17 **KEYWORDS:** RNA transcripts, *de novo* assembly, RNA sequencing, long reads, hybrid assembly

18

19 **RUNNING TITLE:** HyDRA: a new hybrid *de novo* RNA assembly pipeline

20

21

22

23

24

25

26 **ABSTRACT**

27 **Background:** Short-read RNA sequencing (RNAseq) has widely been used to sequence RNA
28 from a wide range of different tissues, developmental stages and species. However, the
29 technology is limited by inherent biases and its inability to capture full-length transcripts. Long-
30 read RNAseq overcomes these issues by providing reads that can span multiple exons, resolve
31 complex repetitive regions and the capability to cover entire transcripts. Unfortunately, this
32 technology is still prone to higher error rates. Noncoding RNA transcripts are highly specific to
33 different cell types and tissues and remain underrepresented in current reference annotations.
34 This problem is exacerbated by the dismissal of sequenced reads that align to genomic regions
35 that do not contain annotated transcripts, resulting in approximately half of the expressed
36 transcripts being overlooked in transcriptional studies.

37 **Results:** We have developed a pipeline, named HyDRA (Hybrid *de novo* RNA assembly), which
38 combines the precision of short reads with the structural resolution of long reads, enhancing the
39 accuracy and reliability of custom transcriptome assemblies. Deep, short- and long-read RNAseq
40 data derived from ovarian and fallopian tube samples were used to develop, validate and assess
41 the efficacy of HyDRA. We identified more than 50,000 high-confidence long noncoding RNAs,
42 most of which have not been previously detected using traditional methods.

43 **Conclusions:** HyDRA's assembly performed more than 40% better than a similar assembly
44 obtained with the top-ranked stand-alone *de novo* transcriptome short-read-only assembly tool and
45 over 30% better than one obtained with the best-in-class multistep short-read-only approach.
46 Although long-read sequencing is rapidly advancing, the vast availability of short-read RNAseq
47 data will ensure that hybrid approaches like the one implemented in HyDRA continue to be
48 relevant, allowing the discovery of high-confidence transcripts within specific cell types and
49 tissues. As the practice of performing hybrid *de novo* transcriptome assemblies becomes
50 commonplace, HyDRA will advance the annotation of coding and noncoding transcripts and
51 expand our knowledge of the noncoding genome.

52

53 **BACKGROUND**

54 Short-read RNA sequencing (RNAseq) has revolutionized the transcriptomic era due to its high-
55 throughput, affordability and low error rates¹. However, a limitation of short-read RNAseq lies in its
56 dependency on fragmenting the original transcript molecules. Reassembling and quantifying these
57 sequenced reads, typically of ~50 to ~500 nt in length, still poses significant computational
58 challenges². The majority of RNAseq studies measure the expression of genes and transcripts
59 by mapping the sequenced reads to a reference annotated transcriptome and removing reads that
60 fail to map. Notably, reference transcriptomes such as those annotated by ENSEMBL and
61 GENCODE are far from complete³, leaving a large proportion of transcripts unquantified by standard
62 RNAseq analysis methods³. To overcome these limitations, a *de novo* custom transcriptome
63 assembly can be performed, to reconstruct the sequenced fragments of transcripts expressed in
64 the sample of interest in substitution of a reference. Mapping sequenced reads onto a custom
65 transcriptome allows the quantitation of expression levels from both annotated and unannotated
66 transcripts⁴. However, to date, only a small fraction of publications make use of *de novo* custom
67 assemblies, accounting for ~1% of the total PubMed publications that use RNAseq. In addition, *de*
68 *novo* assemblies obtained using only short reads cannot accurately resolve all RNA transcripts⁵.

69

70 Long-read sequencing platforms such as those from Pacific Biosciences (PacBio) and Oxford
71 Nanopore Technology (ONT) have the potential to produce full-length transcripts⁶. These
72 platforms can perform end-to-end sequencing of single complementary DNA (cDNA) or RNA
73 molecules, generating long reads that ameliorate the issues caused by transcript
74 fragmentation⁷. ONT platforms include a range of devices in which single molecules thread
75 through a nanopore containing a nanoscale sensor able to detect each nucleotide within a single
76 run⁸. The produced long reads are one order of magnitude longer than typical short reads,
77 providing better resolution of splice junctions, increasing correct isoform identification and the

78 discovery of unannotated transcripts⁸. However, compared to short reads, long reads have much
79 higher base-calling error rates^{7,9,10} and remain a costly and comparatively less used technology.
80 Importantly, although both long-read sequencing and basecaller technologies are continually
81 evolving, most facilities are not equipped to support long-term storage of the large raw data files
82 due to associated costs. Therefore, most users cannot re-call previously sequenced reads when
83 an improved basecalling algorithm is released to increase the quality of long-read data.

84

85 Emerging studies have shown that hybrid transcriptome assembly approaches, which integrate
86 short- and long-read RNAseq data, are more accurate than approaches that use data from
87 either method independently^{11,12,13,14,15,16}. Considering that the average human transcript length
88 is one kilobase (kb)¹⁷ and that long-read sequences are on average 1-3 kb in length^{18,19}, long
89 reads should capture the majority of human transcripts within a single read and ideally bypass
90 the need for reassembly. However, considering the low quality of long reads^{7,9,10}, it is still
91 recommended to correct for intrinsic errors⁹. Although there are different strategies to achieve
92 this, a pre-assembly hybrid error correction using both short and long reads was recently shown
93 to be the best-performing method¹⁰. Additionally, information from both long and short reads
94 may be integrated at the assembly stage, to help reconstruct different isoforms²⁰. To the best
95 of our knowledge, none of the available tools fully benefit from the two types of read integration,
96 but instead adopt either a hybrid-correction-only or a hybrid-assembly-only approach.

97

98 Notably, for long noncoding RNAs (lncRNAs), which constitute the largest class of
99 underrepresented RNA transcripts, their lower abundance in bulk tissues and high content of
100 repetitive elements means the assembly challenge is even more pronounced^{21,22,23}. The few
101 lncRNA-focused hybrid assembly studies that have been performed indicate that RNAseq data
102 integration can enhance the accuracy and reliability of lncRNA discovery^{24,25}. However, no
103 automated method for hybrid *de novo* assembly to date allows for accurate lncRNA discovery.

104

105 To address the need for comprehensive discovery of unannotated transcripts, we developed
106 HyDRA (Hybrid *de novo* RNA assembly), a true-hybrid pipeline that integrates short- and long-
107 read RNAseq data for *de novo* transcriptome assembly, with additional steps for lncRNA
108 discovery. Our pipeline combines read treatment, assembly, filtering and parallel quality control
109 (QC) steps to ensure the reconstruction of high-quality transcripts. Comprehensive tests
110 showed that HyDRA outperforms the current best-in-class short-read-only approach⁴. In
111 contrast with long-read sequencing, a vast amount of short-read RNAseq data is readily
112 available for many species, tissues and conditions. Pipelines like HyDRA can make best use of
113 available data in its totality, allowing users to achieve high-quality transcriptome assemblies
114 while long-read sequencing technologies continue to advance. We anticipate that HyDRA will
115 facilitate the generation of tissue-specific custom transcriptomes, providing a valuable resource
116 for expression analyses across different cell types and tissues.

117

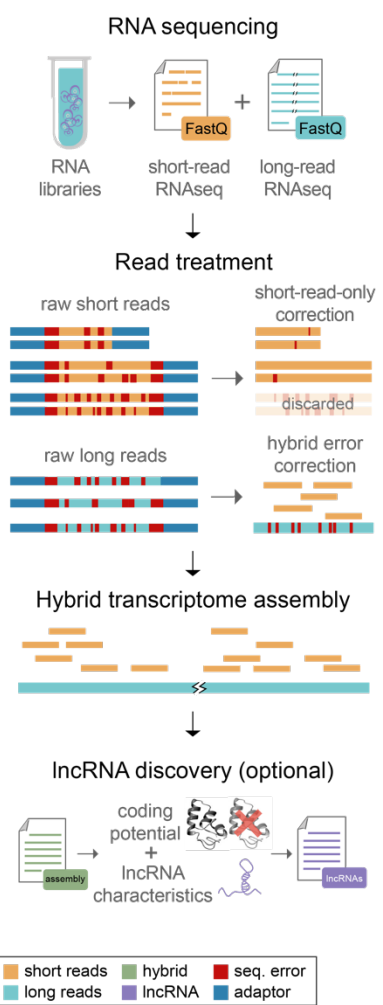
118 RESULTS AND DISCUSSION

119 Overview of the HyDRA pipeline

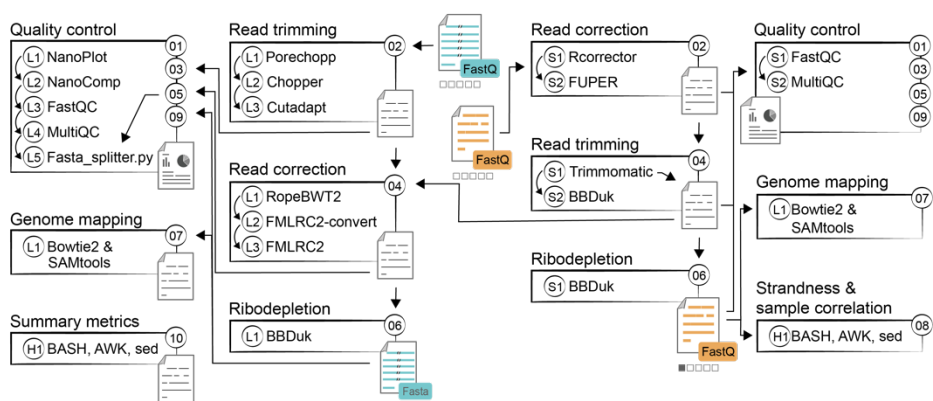
120 We developed HyDRA (Figure 1A), a hybrid pipeline that integrates bulk short- and long-read
121 RNAseq data for generating custom transcriptomes. This is achieved through (i) read treatment
122 steps to correct sequencing errors by treating low-frequency *k*-mers and removing contaminants
123 (e.g. adaptors and reads from ribosomal RNAs), (ii) steps to *de novo* assemble the filtered and
124 corrected reads and further process the resulting assembly, and (iii) optional steps to discover
125 a high-confidence set of lncRNAs supported by multiple machine-learning model predictions
126 (Figure 1B-D). This section and Additional file 1 contain a detailed explanation of HyDRA,
127 including the tools and algorithms underlying each step (Table 1; Additional File 2: Table S1).

128

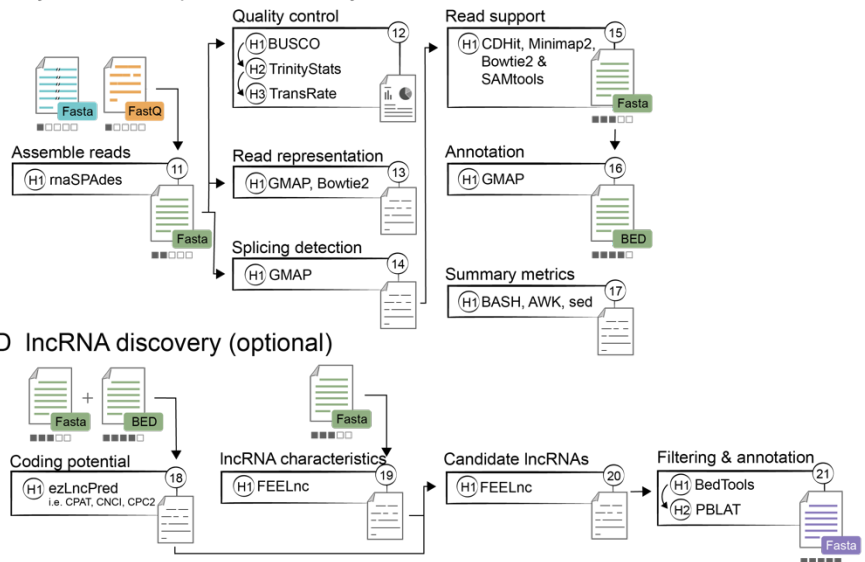
A HyDRA overview



B Read treatment



C Hybrid transcriptome assembly



D IncRNA discovery (optional)

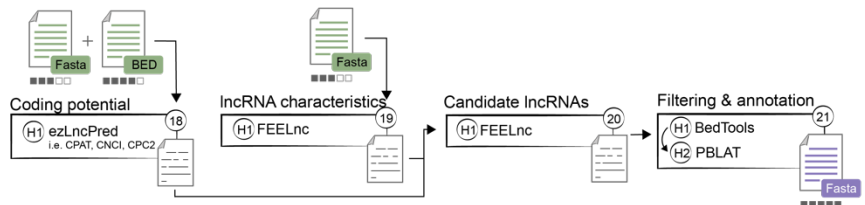


Figure 1

129

130

131 HyDRA. **(A)** Overview of the pipeline, from RNA library preparation to sequencing and
 132 availability of raw fastQ files for both short- and long-read samples. **(B)** Both short and long
 133 reads first undergo extensive quality control and processing, including hybrid error-correction
 134 of long reads and short-read-only correction of short reads. These steps are important to assess
 135 low-frequency *k*-mers for error correction and to remove contaminants (e.g. adaptors and reads
 136 from ribosomal RNAs). Summary metrics for these steps are printed at the end. **(C)** Treated
 137 reads undergo a hybrid *de novo* transcriptome assembly and further filtering and quality
 138 assessment. Summary metrics for these steps are printed at the end. **(D)** Optional steps can
 139 be performed for the discovery of high-confidence IncRNAs.

140

141 **Read treatment**

142 Sequencing errors are known to introduce artificial nodes in de Bruijn graphs during *de novo*
143 isoform resolution²⁶ and interfere with all downstream steps^{27,28}. In addition to correcting
144 sequenced reads, common read processing practice includes removing adaptor sequences
145 identified during the raw quality assessment of the data²⁹. Traditional tools optimized for short-
146 read data fail to correctly treat longer sequences^{7,9,30}. Therefore, HyDRA includes scripts and
147 subroutines carried out by best-performing tools specifically designed to process these data
148 separately (Figure 1B). As a result, HyDRA's read treatment phase includes 38 scripts that
149 perform the first ten steps. The short-read processing steps of HyDRA follow our previously
150 published *de novo* assembly pipeline, which is currently best-in-class⁴. Processed in parallel,
151 long-read treatment steps are dependent on the pre-processed short-reads for hybrid error
152 correction using FMLRC2 v.0.1.7^{10,31}. QC routines are interspersed throughout the read
153 treatment steps to guarantee high read quality, including an in-house Python script
154 (fasta_splitter.py) to assess long-read length, allowing the user to implement personalized cut-
155 offs for ultra-long reads (e.g. > 35 kb). These QC steps were designed to enhance the quality
156 of input read data and are performed after each key processing step.

157

158 ***De novo* assembly**

159 We selected RnaSPAdes v.3.14.1¹² as the assembler for HyDRA, as it was specifically designed
160 for integrating short and long RNAseq reads and is the only available assembler that uses a
161 genome-independent process (Additional file 2: Table S1, Figure 1C). RnaSPAdes was developed
162 from the foundational algorithms SPAdes and hybridSPAdes, enabling the integration of both
163 paired-end short-read RNAseq data and single-end long-reads, from either PacBio or ONT. This
164 approach facilitates the construction of a high-quality transcriptome assembly that represents
165 full-length transcripts and their alternative isoforms¹². Next in the HyDRA pipeline, a step is
166 included to remove highly redundant transcripts and differentiate between multiexonic and

167 monoexonic sequences in the assembly. This allows users to set appropriate read support
168 thresholds for each subset of transcripts, with monoexonic transcripts requiring higher read
169 support to differentiate from sequencing noise or genomic DNA contamination. HyDRA uses
170 reads per kilobase per million (RPKM) values from independent short- and long-read alignments
171 to estimate read support, with user-defined thresholds for filtering.

172

173
$$(i) RPKM = \frac{\text{Read count} \times 10^9}{\text{Total reads} \times \text{Feature length}}$$

174

175 Assembled transcripts are then aligned to the reference transcriptome to identify unannotated
176 transcripts in the custom transcriptome. Similar to our QC routine for input reads, we use a series
177 of biologically supported quality evaluation tools (BUSCO v.20161119³², Trinity Stats v.2.8.4³³ and
178 TransRate v.1.0.3²⁷), to assess completeness and other metrics that characterize the generated
179 custom transcriptome. With that, this section of the pipeline includes 9 scripts performing 7 steps,
180 with 3 additional scripts included for short-read-only assembly and processing.

181

182 ***LncRNA discovery (optional)***

183 A custom transcriptome assembly can help in the discovery of a variety of transcript types, with
184 lncRNAs representing a substantial portion of the unannotated transcriptome. lncRNAs are highly
185 specific to different tissues, cell types and developmental stages^{4,34}. Despite their significance,
186 lncRNAs are often underrepresented in transcriptional studies due to their lack of annotation in
187 reference transcriptomes. This is partially due to short-read RNAseq inherent biases and
188 inability to capture full-length transcripts. Using a combination of long and short reads, HyDRA
189 is well-equipped to facilitate the annotation of lncRNAs. We have therefore included 4 optional
190 steps after the core assembly that allow HyDRA to perform lncRNA discovery. Using a
191 combination of three machine learning models from ezLncPred v.1.0³⁵, i.e. CPAT, CNCI, CPC2,
192 we first predict the coding potential of the transcripts identified in the assembly. These transcripts

193 are then assessed in parallel by FEELnc v.0.2 for lncRNA characteristics³⁶. FEELnc is a suite of
194 machine learning algorithms that requires the user to supply both a reference annotation of protein-
195 coding transcripts and previously annotated lncRNA transcripts (e.g. GENCODE annotation) to
196 train the model to classify transcripts assembled by HyDRA. A transcript is then considered to be a
197 candidate lncRNA based on FEELnc's prediction in combination with the predicted absence of
198 coding potential detected by at least two different ezLncPred tools. To remove false-positive
199 lncRNAs (i.e. transcripts that match annotated protein-coding transcripts), HyDRA maps the
200 candidate lncRNAs to the reference transcriptome. Candidate lncRNAs matching protein-coding
201 transcripts with at least 75% identity and a minimum bidirectional overlap of 85% on either
202 strand, are identified as false-positives and removed. Coordinates of candidate lncRNAs are
203 also intersected with protein-coding genes using BedTools³⁷, resulting in a final set of high-
204 confidence lncRNAs. Finally, HyDRA maps the candidate lncRNAs to a comprehensive database
205 of confirmed lncRNAs that can be the internal default (containing 112,439 lncRNAs from multiple
206 sources, as described in Bitar *et al.* 2023⁴) or a user-defined database. This allows the user to
207 pinpoint which lncRNAs have been detected for the first time in the custom assembly, and which
208 were already known, either from the reference transcriptome or from additional databases
209 (Additional file 1).

210

211 **HyDRA improves the quality of both short- and long- sequenced reads**

212 HyDRA was developed and tested using data obtained from short- and long-read RNAseq on
213 primary and immortalized fallopian tube secretory epithelial cells (FTSEC) and ovarian surface
214 epithelial cells (OSEC) (Additional file 2: Table S2). QC of raw RNAseq data confirmed an
215 expected high median Phred quality of 35.65 for the short-read data, and a median quality of
216 12.90 for the long-read data (Additional file 2: Table S3; Additional file 3: Figures S2-S3). We
217 used the Illumina NovaSeq™ 6000 for short read sequencing, which has the lowest error rates
218 for high-throughput sequencing³⁸. For long-read sequencing, we used ONT with current error

219 rates predicted at 5-10%^{9,39}. Common practice with long read RNA sequencing includes the
220 removal of reads below a mean minimum Phred quality of 7 (Q7), which is a much lower
221 threshold than for short-read data. In our dataset, all long-reads were over Q7, with 93% of
222 them surpassing Q10 (Additional file 2: Table S3).

223

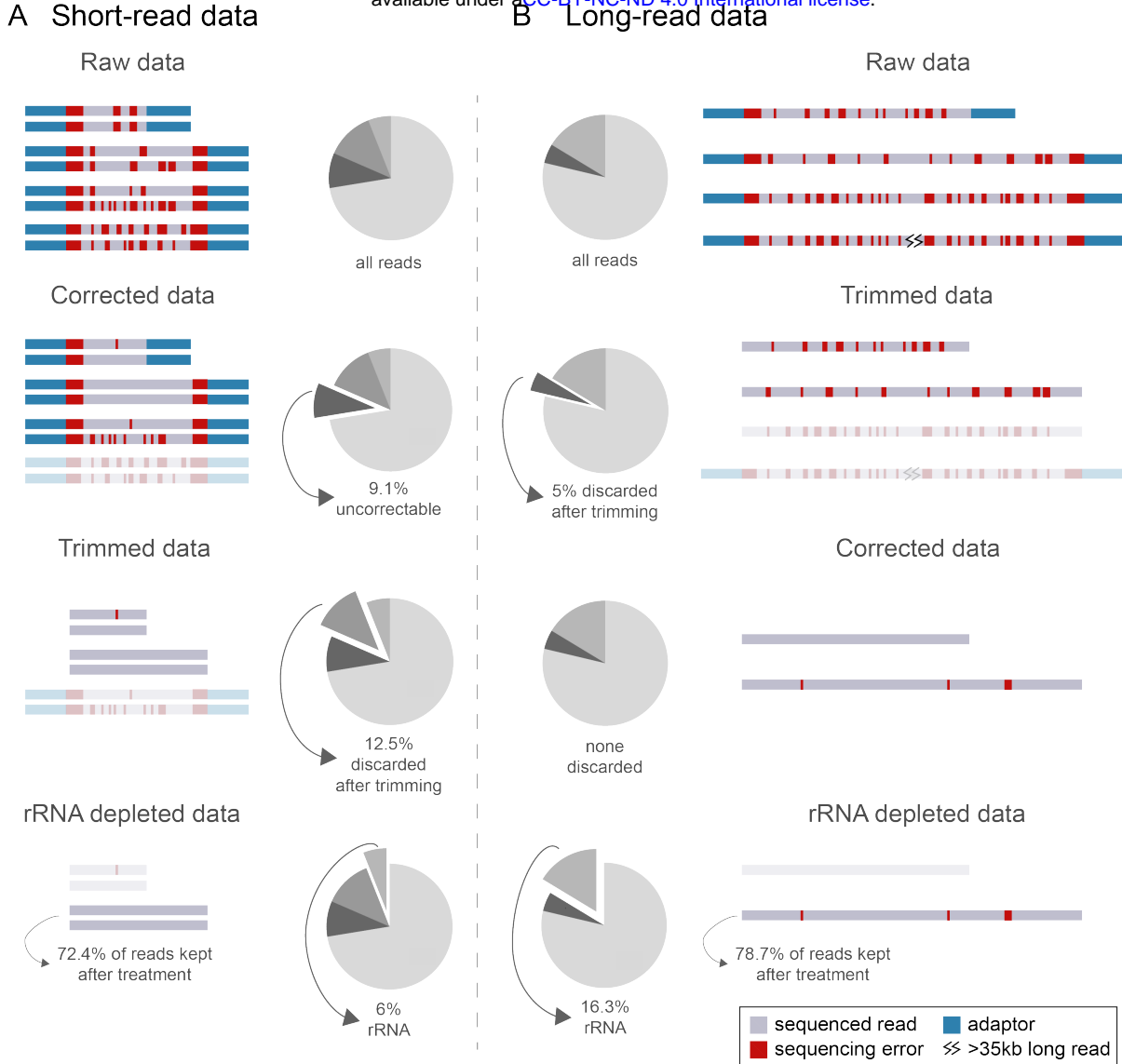
224 The short-read treatment steps begin with correction of raw reads and subsequent trimming.
225 The majority of the short reads survived the correction step (average of 9.16% uncorrectable
226 reads; Figure 2; Additional file 2: Table S3; Additional file 4) and about 60% of the sequence
227 ends were above the minimum quality set for trimming Q30 (Additional file 2: Table S3),
228 indicating a high quality of corrected and trimmed short reads. Median short-read quality
229 measured in the Phred scale increased from 35.65 to 36.12 after treatment steps were
230 performed (Additional file 3: Figure S1-S2; Additional file 2: Table S3), with a concomitant
231 decrease in the calculated error rate from 1 base in ~3,000 to 1 in ~4,000. In HyDRA, due to
232 the prerequisites of the selected tools, the long-read treatment steps follow the opposite order,
233 with trimming (adaptor removal followed by quality trimming) performed before correction.
234 Median long-read quality measured in the Phred scale showed an increase from 12.90 to 14.50
235 after trimming. Approximately 5% of the reads were discarded during adaptor removal and
236 quality trimming (Figure 2). From the remaining reads, 99% were above Q10 and 81% were
237 above Q12 (Additional file 3: Figure S3; Additional file 2: Table S3). Next, we integrated the pre-
238 processed short- and long-read sequencing data to perform the hybrid error correction. We
239 observed a balanced base composition in the Burrows-Wheeler transform created from all pre-
240 processed short reads. However, we consistently noticed that RopeBWT²⁰, one of the tools
241 used in the hybrid error correction steps (more details on Additional file 1) outputs a base count
242 report in which thymine base counts and N (undefined) base counts are swapped. This has
243 been addressed in HyDRA which now outputs the correct base counts to the user (Additional
244 file 2: Table S3). Despite base quality information being lost after long-read correction, no

245 sequences were discarded at this point, implying that all reads that survived trimming were
246 corrected and kept for further processing (Additional file 2: Table S3).

247

248 Most RNAseq library preparation protocols include a ribodepletion or poly(A) selection step, but
249 ribosomal RNAs (rRNAs) still represent a large portion of the sequenced data²⁹. These are
250 considered cognate contaminants, meaning they are reads originating from undesired RNA
251 types and must be removed prior to the *de novo* assembly. Using a database of known rRNAs
252 sequences (Additional file 2: Table S1), we have included a step in HyDRA where pre-
253 processed reads are computationally filtered to remove ribosomal contamination. During quality
254 assessment with FastQC, two long-read sequences identified as overrepresented were
255 confirmed through BLAT searches to be human rRNAs⁴⁰. On average, short-read data
256 contained 6.00% of rRNA-derived reads and long-read data contained 16.30% (Figure 2;
257 Additional file 2: Table S3). These numbers align with expected rRNA sequencing levels, even
258 after ribodepletion during library preparation⁴¹.

259



260

261 Figure 2

262 Short- and long-read data treatment in HyDRA. **(A)** Paired-end short-read data, followed by pie
263 charts highlighting the proportion of reads discarded in each step relative to the total number of
264 raw reads. **(B)** Single-end long-read data, preceded by pie charts highlighting the proportion of
265 reads discarded in each step relative to the total number of raw reads.

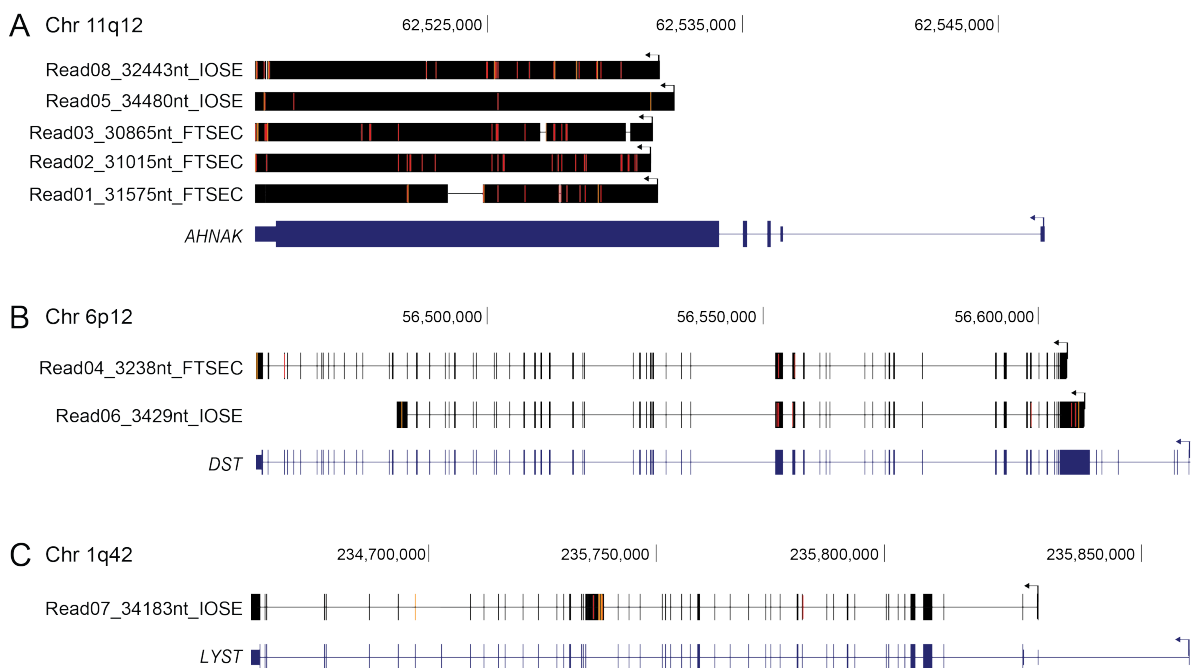
266

267 Long-read sequences of up to 35 kb were kept and used for assembly

268 The longest known human transcript is *TTN* (titin), with 109,224 nt⁴², thus we anticipated that
269 certain long-read sequences in our dataset would be significantly longer than the reported
270 average of 1-3 kb^{18, 19}, potentially including ultra-long reads over 100 kb in length. Indeed.

271 although the average length of the raw long reads was 1024 nt, the longest was 103,744 nt
272 (Additional file 3: Figure S4A-C; Additional file 2: Table S3). FastQC analysis indicated that,
273 while reads with up to ~30,000 nt had the expected base composition (i.e. balanced proportions
274 of A, T, C and G), longer sequences presented a distinctively biased pattern of nucleotide
275 composition, rich in thymines and guanines (Additional file 3: Figure S4B). In light of this, we
276 implemented an additional QC routine to analyze sequence lengths throughout the pipeline and
277 allow users to remove sequences with unexpected nucleotide composition (fasta_splitter.py;
278 Additional file 3: Figure S4D). After all read treatment steps were performed, the eight remaining
279 longest sequenced reads (Additional file 2: Table S3; 30-35 kb), were aligned to the GRCh38
280 reference genome using BLAT⁴⁰ (Figure 3). All were confirmed as valid human sequences,
281 aligning to *AHNAK* (desmoyokin), *DST* (dystonin) or *LYST* (lysosomal trafficking regulator). All
282 treated long-read sequences were used for *de novo* assembly, including those reaching 35 kb.
283 Importantly, this maximum length is dependent on the input data, the tissue(s), developmental
284 stage and species being analyzed. Additionally, through fasta_splitter.py, HyDRA gives users
285 the option to strictly keep sequences that have up to *n* nt in length.

286



287

288 **Figure 3**

289 Treated long-read sequences reaching up to 35 kb aligned to the human genome using BLAT.
290 These eight pre-processed reads (four from FTSEC and four from OSEC samples) were aligned
291 against the human genome (GRCh38) in a UCSC BLAT search to confirm they were valid
292 sequences. The sequencing reads that aligned to **(A) AHNAK**, **(B) DST** or **(C) LYST**.

293

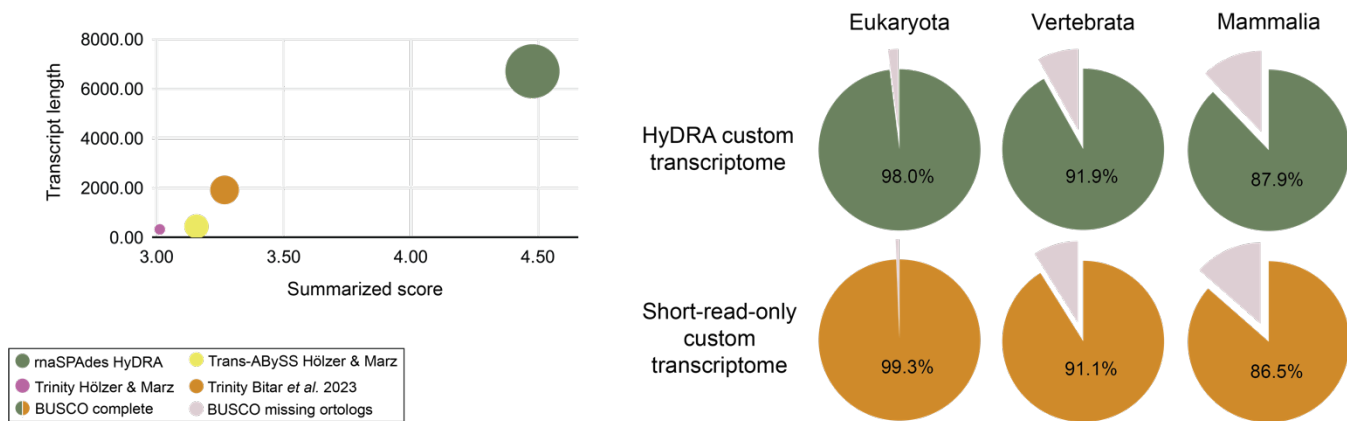
294 **Hybrid transcriptome assembly performs better than short-read-only approaches**

295 To assess HyDRA's assembly, a short-read-only assembly was created by combining the treated
296 short reads as an input for Trinity v.2.8.4³³ with normalized read coverage at 50 to prevent
297 fragmented transcripts⁴. This assembly was subjected to the same processing steps as the hybrid
298 counterpart. To evaluate the quality of both assemblies, we used a subset of the metrics reported
299 in a recent benchmark study and respective normalized score (0-1)⁴³. These metrics included
300 transcript length, N50, reference coverage, open reading frame (ORF) percentage, undefined
301 base count and conserved orthologs representation. Based on the normalized score, the
302 HyDRA generated assembly performed 31% better than the best performing short-read-only
303 approach⁴, and outperformed the top-ranked *de novo* assembly tool alone by 41% (Figure 4A;
304 Additional file 2: Table S4)⁴³. Our hybrid approach generated 857,736 transcript sequences,
305 reaching up to 67,466 nt, with an average transcript length of 2,409 nt and GC content of ~44%
306 (Additional file 2: Table S4), which aligns with the reported human GC content of coding (~52%)
307 and noncoding (~44%) isoforms⁴⁴.

308

A Summarized metric (0-1) assembly scores

B Recapitulated human orthologs



309

310 **Figure 4**

311 Overall assessment of the HyDRA-generated assembly. **(A)** Normalized assembly scores.
312 Bubbles sizes vary according to N50 value. The graph shows scores for the assemblies
313 produced by i) the best (Trans-ABYSS) and second best *de novo* assembly tools alone
314 (Trinity)⁴³; iii) Bitar *et al.* 2023⁴ pipeline; iv) HyDRA. Both (i) and (ii) were based on data
315 described by Hölzer and Marz's⁴³ and (iii) and (iv) based on data described here (from human
316 ovarian and fallopian tube samples). **(B)** HyDRA's assembly completeness from BUSCO
317 analysis.

318

319 In terms of assembly contiguity, N50 is an important metric defined as the length of the
320 sequence at which 50% of the total assembly size is contained in sequences of at least that
321 length. HyDRA produced an assembly with N50 of 6708 nt, which reflects how a hybrid
322 approach can represent full-length human transcripts (Additional file 2: Table S4). For
323 comparison, Hölzer and Marz's best performing assembler produced a transcriptome with an
324 N50 of 441 nt (15.21 times smaller than HyDRA's assembly)⁴³ and Bitar *et al.* 2023 an N50 of
325 1383 (4.85 times smaller than HyDRA's assembly)⁴. The highest N50 observed by Hölzer and
326 Marz⁴³ was 2381 nt (2.82 times smaller than HyDRA's assembly), but this study showed that
327 the assembler performed poorly compared to the other tools and metrics. To investigate the
328 contribution of adding long reads to transcriptome assembly, we used the Bitar *et al.* 2023⁴

329 pipeline to create an assembly based only on our short-read data, comparing it with HyDRA's
330 hybrid assembly. The calculated N50 of the short-read-only assembly was three times smaller
331 than HyDRA's and the assembly had double the number of transcripts. This suggests HyDRA
332 can generate less fragmented assemblies, that are likely to better recapitulate full-length
333 transcripts, while maintaining high overall quality. Similar to the N50, the N90 metric
334 corresponds to the transcript length at which 90% of the total assembly size is contained in
335 sequences of at least that length. Using our hybrid approach, we achieved an N90 of ~1000 nt,
336 meaning that 90% of the transcripts in the HyDRA assembly are sequences matching the
337 average human transcript length¹⁷. This demonstrates the overall contiguity of the produced
338 custom transcriptome (Additional file 3: Table S4).

339

340 The HyDRA-generated assembly accurately recapitulated several aspects of the human
341 transcriptome. For example, BUSCO analysis revealed > 98% of the eukaryotic (297/303),
342 91.9% of the vertebrata (2376/2586) and 87.8% of the mammalian (3606/4104) conserved
343 orthologs were captured in our hybrid assembly, indicating overall completeness (Figure 4B).
344 These values were similar to those obtained from the short-read-only assembly (Additional file
345 2: Table S4). According to TransRate, the custom hybrid assembly covered 24% of the
346 reference human transcriptome (GENCODE), which is comparable to the 23-26% observed in
347 the best performing assembler tools found by Hölzer and Marz⁴³ (Additional file 2: Table S4).
348 For perspective, HyDRA's transcripts cover approximately 12% of the reference genome while
349 the exons and UTRs in the reference annotation (GENCODE v36) cover approximately 5%
350 (genome coverages were calculated with BedTools genomecov).

351

352 **Splicing assessment showed 30% of transcripts to be multiexonic**

353 Most assemblies to date disregard monoexonic transcripts, but recent evidence has shown this
354 class contains conserved lncRNAs of functional relevance^{45,46,47,48}. Similar to Bitar *et al.* 2023⁴,

355 we have kept the monoexonic transcripts in our assembly, as long as they had high read
356 support. Transcripts aligned to the reference human genome (GRCh38) were classified as
357 monoexonic or multiexonic according to the presence of 'N' tags in the alignment file. A minimum
358 length of 50 nt was defined to differentiate introns from insertions and deletions (indels), which
359 aligns with current knowledge about human introns. Before filtering out low read support
360 transcripts, our hybrid assembly showed a ratio of multiexonic:monoexonic transcripts of 3:7
361 (~232,000 transcripts were classified as multiexonic and ~619,000 as monoexonic; Figure 4C;
362 Additional file 2: Table S4). For comparison, the short-read-only approach showed a ratio of
363 3:17 (~143,000 were multiexonic and ~740,000 were monoexonic), likely reflecting the power
364 of long reads to resolve transcript architecture and improve overall isoform assembly.

365

366 Removing transcripts with low read support helps remove technical artifacts and transcriptional
367 leakage products, as well as problematic transcripts arising from misassembly. As HyDRA
368 integrates short and long reads, read support for each transcript was calculated based on a
369 combination of both subsets, which is computationally and biologically challenging. In HyDRA,
370 redundant transcripts are collapsed prior to read support calculations. This redundancy
371 reduction step removed ~8,500 transcripts from the original assembly (Additional file 2: Table
372 S4). From the remaining ~224,500 multiexonic and ~618,000 monoexonic transcripts, ~189,000
373 (84.34%) and ~13,000 (2.12%) respectively, passed the more permissive RPKM cut-off for read
374 support (0.3 and 3 RPKM). As expected, the number of supported transcripts was much lower
375 when using the stricter RPKM cut-off (1 and 5 RPKM), with a 90% decrease in multiexonic
376 (~20,000) and 50% decrease in monoexonic transcripts (~7,300) passing the filtering step.
377 Since we previously validated transcripts with low read support by qPCR, confirming that the
378 less stringent cut-off still identifies bona fide transcripts⁴, we opted to use these transcripts for
379 further analysis. The ratio of multiexonic to monoexonic transcripts in the assembly is 1:14,
380 maintaining the expected lncRNA ratio observed in the Telomere-To-Telomere (T2T) human

381 genome (T2T-CHM13). In total, the final filtered custom assembly consists of 202,459
382 transcripts, providing a comprehensive representation of the normal ovarian and fallopian tube
383 transcriptome.

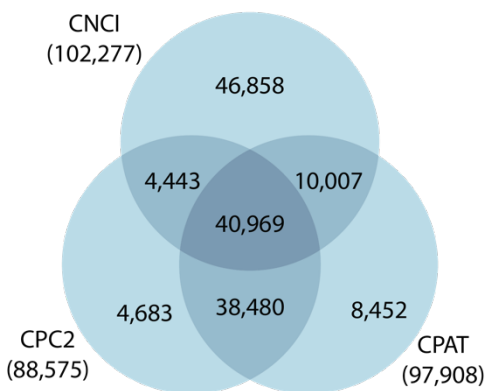
384

385 **Identification of unannotated lncRNAs in HyDRA's custom transcriptome**

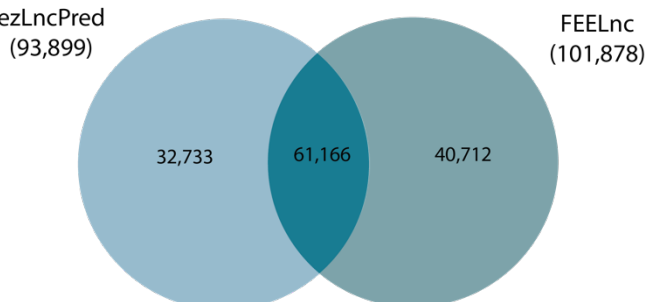
386 To assess the coding potential of the 202,459 transcripts, we ran three machine learning models
387 from the ezLNCpred package, CPAT, CNCI and CPC2³⁵. On average, at least two of the models
388 agree on 61% of the noncoding predictions (93,899), suggesting that these methods are more
389 effective at confirming the absence of ORFs rather than detecting their presence. Additionally,
390 26.6% (40,969) had no coding potential detected by any of the three models (Figure 5A;
391 Additional file 2: Table S5). A total of 47,281 transcripts were predicted by at least two models
392 as noncoding and not by any model as protein-coding. We decided to include all 93,899
393 transcripts predicted as noncoding by at least two of the tools in our further analysis (Figure 5B;
394 Additional file 2: Table S5).

395

A Noncoding potential



B lncRNA characteristics



396

397 **Figure 5**

398 LncRNA discovery. **(A)** Intersection of lncRNA candidates predicted by three different
399 ezLNCpred machine learning models (CNCI, CPAT and CPC2). **(B)** Intersection between
400 FEELnc lncRNA predictions and the list of candidates predicted by at least two of the ezLNCpred
401 machine learning models.

402

403 FEELnc was trained using the GENCODE GRCh38 transcriptome annotation of protein-coding
404 and lncRNA transcripts⁴⁹. This enabled us to identify which of the 202,459 transcripts
405 assembled by HyDRA had lncRNAs characteristics. To ensure robust predictive capability, we
406 exclusively used experimentally validated GENCODE lncRNAs. FEELnc predicted 101,878
407 transcripts to be lncRNAs (Additional file 2: Table S5). This represents about half of the total
408 number of transcripts in our custom transcriptome, indicating that lncRNAs constitute a
409 significant proportion of expressed transcripts in normal ovarian and fallopian tube tissues.
410 Importantly, more than 60% of these (61,166) lncRNAs were supported by at least two of the
411 three ezLncPred machine-learning models (Figure 5B).

412

413 The majority of these candidate lncRNAs were multiexonic, which may reflect the biased
414 training dataset. From the 61,166 candidate lncRNAs, 629 showed a bidirectional overlap of at
415 least 85% with a protein-coding transcript and a minimum identity of 75%. We believe these to
416 be either false-positives that our methods failed to detect, or noncoding isoforms of protein-
417 coding genes. Although monoexonic and sense genic transcripts (i.e. those overlapping
418 protein-coding genes in the same strand) are functionally relevant, it is difficult to differentiate
419 these from technical artifacts or transcriptional leakage. Furthermore, sense genic lncRNAs
420 cannot easily be uncoupled from the corresponding protein-coding gene, and we have included
421 a restrictive alignment step to facilitate their removal. From the remaining 60,537 lncRNAs, 228
422 were already annotated in GENCODE (GRCh38: 19 multiexonic; 1 monoexonic) or known to
423 the database of over 112,000 lncRNA transcripts (124 multiexonic; 84 monoexonic). We also
424 intersected the coordinates of the remaining 60,309 lncRNAs with those of protein-coding
425 genes using BedTools³⁷. This allowed us to further remove 7,615 exon-overlapping transcripts,
426 resulting in the identification of 53,551 high-confidence lncRNA transcripts. Importantly, HyDRA
427 was designed to split monoexonic and multiexonic sequences after assembly, which allows

428 users to easily focus on either or both sets of transcripts.

429

430 To demonstrate the functional relevance of these 53,551 high-confidence lncRNA transcripts
431 from the normal ovaries and fallopian tubes, we assessed their expression profiles in a different
432 subset of sequenced RNA samples (unrelated but biologically similar to those used for
433 assembly). We used publicly available RNAseq data from normal and cancerous ovarian and
434 fallopian tube tissues found in the RNA Atlas project⁵⁰. This revealed that 27,257 (44.56%)
435 lncRNAs were expressed in at least one of the samples, demonstrating HyDRA's efficient
436 assembly of both annotated and unannotated lncRNA transcripts, through the integration of
437 long- and short-read RNAseq data.

438

439 CONCLUSIONS

440 Here we present HyDRA, a comprehensive pipeline that integrates short- and long-read
441 sequencing data for a true-hybrid *de novo* transcriptome assembly and lncRNA discovery. We
442 used deep, short- and long-read RNAseq from ovarian and fallopian tube epithelial cells
443 samples to develop, validate and assess the efficacy of the pipeline in generating a high-quality
444 custom transcriptome. We have shown that HyDRA's assembly performed > 40% better than
445 the top-ranked stand-alone *de novo* transcriptome assembly tool and > 30% better than our
446 recent best-in-class short-read-only approach⁴. Based on this custom assembly, we identified
447 61,166 candidate lncRNAs, among which 60,309 have not been previously annotated and
448 53,551 showed no overlap with protein-coding transcripts. In summary, HyDRA is a high-
449 performing hybrid-assembly tool capable of facilitating accurate transcriptome reconstruction
450 and advancing lncRNA annotation.

451

452 **MATERIALS AND METHODS**

453 **RNAseq sample preparation and sequencing**

454 RNA was extracted from primary and immortalized fallopian tube secretory epithelial cells
455 (FTSEC) and ovarian surface epithelial cells (OSEC) using the QIAGEN RNeasy Plus Mini kit
456 (Additional file 2: Table S2). One microgram of total RNA was rRNA depleted with the Ribo-
457 Zero™ Plus kit according to the manufacturers' instructions (Illumina). Short-read RNAseq
458 libraries were prepared using the Truseq Stranded mRNA Library Prep Kit (Illumina), and
459 sequenced at high depth (PE150, > 75 million reads per sample; Additional file 2: Table S2) on
460 the Illumina Novaseq™ 6000 (Australian Genome Research Facility, Melbourne, Australia).
461 High sequence depth is considered best practice for lncRNA discovery, as they are often
462 expressed at low levels and have poor isoform representation⁵¹. For long-read sequencing,
463 cDNA was extracted from one FTSEC and one OSEC cell line (Additional file 2: Table S2).
464 ONT cDNA libraries were generated with polyadenylation enrichment and SQK-NBD114.24
465 native barcoding kit at the Garvan Institute's Nanopore Sequencing Facility (Australia).
466 Samples were barcoded using the supplied PCR barcodes and sequenced at high depth (> 69
467 million reads per sample; Additional file 2: Table S2) on the PromethION™ P48 flowcells (FLO-
468 PRO114M - R10.4.1). The slow5 files were base-called using Guppy v.6.4.6+ae70e8f and
469 MinKNOW v.22.12.5 by the Garvan Institute's Nanopore Sequencing Facility (Australia).

470

471 **Databases and reference genome versions**

472 We used the human genome GCRh38 release 79⁴⁹ for lncRNA identification and annotation),
473 and the T2T-CHM13 genome⁵², for long-read effects on the produced transcriptome assembly.
474 The GENCODE annotation for GCRh38 was used as the reference transcriptome. A previously
475 published database of 169 human rRNA sequences⁴, with the addition of two sequences
476 identified from our FastQC analysis (Additional file 2: Table S2), was used to filter pre-
477 processed reads for ribosomal contamination. To identify which of the discovered lncRNAs

478 were known and which were novel, we used all annotated lncRNAs in GENCODE GRCh38
479 together with a comprehensive database of > 112,000 known lncRNA genes from 8 public
480 repositories (BIGtranscriptome, MiTranscriptome and LNCipedia from lncRNAB53; Cabili *et al.*
481 2011⁵⁴; CancerSEA⁵⁵; Lanzos *et al.* 2017⁵⁶; LncRNADisease⁵⁷ and RNACentral⁵⁸), as
482 described in Bitar *et al.*⁴. Experimentally confirmed protein-coding and lncRNAs annotated in
483 the same GENCODE version were used to train the machine-learning algorithms FEELncfilter,
484 FEELnc_codpot and FEELnc_classifier³⁶.

485

486 **Parameters used for the ovarian and fallopian tube custom assembly**

487 A comprehensive list of the parameters used in each step is available in Additional file 2: Table
488 S1). Importantly, we defined both a restrictive and permissive set of cut-offs for read support. A
489 strict read support of 3 RPKM was enforced for monoexonic transcripts, but we relaxed the cut-
490 off to 0.3 RPKM for multiexonic transcripts. This is in agreement with⁴ and maintained the
491 expected ratio of multiexonic to monoexonic lncRNAs of 14:1, consistent with annotations based
492 on the T2T genome. A stricter threshold of 5 RPKM and 1 RPKM, respectively, was also tested.
493 Importantly, lncRNAs expressed at ~0.5 RPKM had previously been experimentally confirmed
494 by our group with an 80% success rate⁵⁹.

495

496 **Expression profiles of lncRNA transcripts**

497 RNAseq analysis was run based on the GRADE (General RNAseq Analysis for Differential
498 Expression) pipeline⁴. Modifications to these scripts now allow the user to quantify reads based
499 on any user-provided transcriptome sequence and are available at⁶⁰. The expression profiles of
500 lncRNAs were assessed in (i) ovarian and fallopian tube whole tissue; (ii) high-grade serous ovarian
501 carcinoma (HGSOC) tumor samples, including homologous recombination (HR)-deficient and HR-
502 proficient; and (iii) HGSOC cell lines. Public RNAseq of ovarian and fallopian tube samples,
503 sequenced at high depth, were obtained from the RNA Atlas project⁵⁰.

504

505 **Bioinformatics tools used for HyDRA development**

506 Our pipeline integrates the currently available open-source tools in BASH scripts using basic UNIX
507 commands to write and submit portable batch system (PBS) jobs. Our scripts were designed to run
508 in a high-performance computer (HPC) where computational tasks are allocated in a PBS. However,
509 general command lines are also available for users that wish to run the pipeline on a different system
510 (See Availability of Data and Materials). Resources used for pipeline development are indicated in
511 each script and can be controlled by the user according to their available computational power. The
512 length evaluation script, `fasta_splitter.py`, was developed in Python 2.7+. To assess HyDRA's
513 assembly, a short-read-only assembly was created by combining the treated short reads as an
514 input for Trinity 2.8.4³³ with normalized read coverage at 50 to prevent fragmented transcripts⁴.

515

516 HyDRA was developed from 39 open-source tools and runs through BASH scripts (Table 1). A
517 comprehensive list of the all tools used in each step is available in Additional file 2: Table S1).
518 BLAT (BLAST-like alignment tool implemented at the UCSC genome browser) searches⁴⁰ were
519 performed to confirm rRNA sequences, long-read sequences and investigate identified lncRNAs.
520 Plots were produced either directly by the underlying tools (referenced in text), with Python 2.7+
521 script available at HyDRA GitHub repository⁶¹). Venn Diagrams were generated with InteractVenn⁶².
522 Figures were edited in Adobe Illustrator v.28.5.

Step(s)	Tool	Version	Source
01L1, 03L1	NanoPlot	1.41.6	⁶³
01L2, 03L2	NanoComp	1.41.6	⁶³
01L3, 01S1, 03L3, 03S1, 05S1, 09S1	FastQC	0.12.1	⁶⁴
01L4, 01S2, 03L4, 03S2, 05S2, 09S2	MultiQC	1.14	⁶⁵
01L5, 03L5, 05L1, 09L1	Fasta_splitter.py	v1.0.6	in house
01L5, 03L5, 05L1, 09L1, 11H1, 14H1, 15H2, 21H2	seqtk	1.3	⁶⁶
02L1	Porechop	0.2.4	⁶⁷
02L2	Chopper	0.5.0	⁶³
02L3	Cutadapt	3.9.13	⁶⁸
02S1	Rcorrector	1	⁶⁹
02S1	Reformat	39.01	⁷⁰
02S2	FilterUncorrectablePEfastq.py	2016	⁷¹

04L1	RopeBWT2	r187	20
04L2, 04L3	FMLRC2	0.1.7	31
04S1	Trimmomatic	0.36	72
04S2, 06L1, 06S1	BBDuk	39.01	70
07L1, 07S1, 13H1, 13H2, 15H1, 15H2	Bowtie2	2.2.9	73
07L1, 07S1, 11H2, 12H2, 13H1, 13H2, 15H1, 15H2, 16H1, 19H1	SAMtools	1.9	74
08L1, 08S1	RSeQC	2.6.4	75
08S2	DeepTools2	3.5.0	76
11H1	RnaSPAdes	3.14.1	12
12H1	BUSCO	20161119	32
12H1	BLAST	2.2.31+	77
11H2, 12H2	Trinity	2.8.4	33
12H3, 12H4	TransRate	1.0.3	27
12H3, 12H4	Fastq-pair	20231003	78
13H1, 14H1, 16H1	GMAP	2023-07-20	79
13H1, 13H2	Picard	2.19.0	80
15H1, 19H1	Minimap2	2.26	81
15H1, 15H2	CD-HIT	4.6.8	82
16H1	Bedops	2.4.41	83
16H1, 18H1, 19H1, 21H1	BedTools	2.29.0	37
18H1	ezLncPred	1.0	35
19H1	UCSC Tools	20160223	84
19H1	FEELnc	0.2	36
21H1	HTSlip	1.19.1	85
21H1	gtf2gff	0.1	86
21H1	genestats	1.0	in house
21H2	PBLAT	2.5.1	87

523

524 **Table 1**

525 Open-source tools used in HyDRA. Steps are arranged in subroutines specific for long reads (L),
526 short reads (S) and hybrid (H).

527

528 **SUPPLEMENTARY INFORMATION**

529 Additional file 1: Complete HyDRA pipeline description

530 Additional file 2: Tables S1-S5

531 Additional file 3: Figures S1-S4

532 Additional file 4: Pipeline validation

533

534 **AUTHORS CONTRIBUTIONS**

535 I.A. and M.B. designed and directed the study and interpreted the data. I.A. developed the
536 pipeline, performed all dry-lab analyses, critically reviewed the computational code, created
537 and maintains the GitHub repository. X.L. prepared the RNA for short- and long-read RNA
538 sequencing. I.A., J.D.F., S.L.E., and M.B. conceived the project and wrote the manuscript with
539 contributions from all authors.

540

541 **FUNDING**

542 This work was supported by grants from the National Health and Medical Research Council of
543 Australia (NHMRC; 2019101) and The Donald and Joan Wilson Foundation. I.A. was supported
544 by a QIMR Berghofer International PhD scholarship and a University of Queensland (UQ)
545 Research Training scholarship. J.D.F. was supported by an NHMRC Investigator Grant
546 (2016826).

547

548 **AVAILABILITY OF DATA AND MATERIALS**

549 The HyDRA pipeline in source and executable form is available without charge for nonprofit,
550 academic, and personal uses under an MIT license at the HyDRA GitHub repository HyDRA⁶¹
551 Zenodo. HyDRA was developed using a x86_64 GNU/Linux operational system in a HPC
552 environment. Expression profiles of lncRNAs discovered from the hybrid custom transcriptome
553 assembly produced were obtained with GRADE2 (General RNAseq Analysis for Differential
554 Expression, version 2), an open-source pipeline under an MIT license and publicly available on
555 GitHub⁶⁰ and Zenodo. Raw short and long RNAseq data generated in this study have been
556 deposited in the National Center for Biotechnology Information's Gene Expression Omnibus
557 (GEO) and are accessible through GEO series accession number XXX000000. Previously
558 published total RNAseq data from the RNA Atlas project under GEO series accession number
559 GSE138734⁵⁰ has been used to perform RNAseq analysis (SRR accession codes are available at

560 Additional file 2: Table S2).

561

562 COMPETING INTERESTS

563 The authors declare that they have no competing interests.

564

565 REFERENCES

- 566 1. Hu, T., Chitnis, N., Monos, D. & Dinh, A. Next-generation sequencing technologies: An overview. *Hum Immunol* **82**, 801-811 (2021).
- 567 2. Garber, M., Grabherr, M.G., Guttman, M. & Trapnell, C. Computational methods for transcriptome annotation and quantification using RNA-seq. *Nat Methods* **8**, 469-77 (2011).
- 568 3. Wu, P.Y., Phan, J.H. & Wang, M.D. Assessing the impact of human genome annotation choice on RNA-seq expression estimates. *BMC Bioinformatics* **14 Suppl 11**, S8 (2013).
- 569 4. Bitar, M. *et al.* Redefining normal breast cell populations using long noncoding RNAs. *Nucleic Acids Res* **51**, 6389-6410 (2023).
- 570 5. Foord, C. *et al.* The variables on RNA molecules: concert or cacophony? Answers in long-read sequencing. *Nat Methods* **20**, 20-24 (2023).
- 571 6. Carbonell Sala, S., Uszczyńska-Ratajczak, B., Lagarde, J., Johnson, R. & Guigó, R. Annotation of Full-Length Long Noncoding RNAs with Capture Long-Read Sequencing (CLS). *Methods Mol Biol* **2254**, 133-159 (2021).
- 572 7. Dong, X. *et al.* Benchmarking long-read RNA-sequencing analysis tools using in silico mixtures. *Nat Methods* **20**, 1810-1821 (2023).
- 573 8. Workman, R.E. *et al.* Nanopore native RNA sequencing of a human poly(A) transcriptome. *Nat Methods* **16**, 1297-1305 (2019).
- 574 9. Amarasinghe, S.L. *et al.* Opportunities and challenges in long-read sequencing data analysis. *Genome Biol* **21**, 30 (2020).
- 575 10. Zhang, H., Jain, C. & Aluru, S. A comprehensive evaluation of long read error correction methods. *BMC Genomics* **21**, 889 (2020).
- 576 11. Shumate, A., Wong, B., Pertea, G. & Pertea, M. Improved transcriptome assembly using a hybrid of long and short reads with StringTie. *PLoS Comput Biol* **18**, e1009730 (2022).
- 577 12. Prjibelski, A.D. *et al.* Extending rnaSPAdes functionality for hybrid transcriptome assembly. *BMC Bioinformatics* **21**, 302 (2020).
- 578 13. Fu, S. *et al.* IDP-denovo: de novo transcriptome assembly and isoform annotation by hybrid sequencing. *Bioinformatics* **34**, 2168-2176 (2018).
- 579 14. Puglia, G.D. *et al.* Hybrid transcriptome sequencing approach improved assembly and gene annotation in Cynara cardunculus (L.). *BMC Genomics* **21**, 317 (2020).
- 580 15. Kainth, A.S., Haddad, G.A., Hall, J.M. & Ruthenburg, A.J. Merging short and stranded long reads improves transcript assembly. *PLoS Comput Biol* **19**, e1011576 (2023).
- 581 16. Vilperte, V. *et al.* Hybrid de novo transcriptome assembly of poinsettia (Euphorbia pulcherrima Willd. Ex Klotsch) bracts. *BMC Genomics* **20**, 900 (2019).
- 582 17. Sharon, D., Tilgner, H., Grubert, F. & Snyder, M. A single-molecule long-read survey of the human transcriptome. *Nat Biotechnol* **31**, 1009-14 (2013).
- 583 18. Xia, Y. *et al.* TAGET: a toolkit for analyzing full-length transcripts from long-read sequencing. *Nat Commun* **14**, 5935 (2023).
- 584 19. Schwenk, V. *et al.* Transcript capture and ultradeep long-read RNA sequencing (CAPLRseq) to diagnose HNPCC/Lynch syndrome. *J Med Genet* **60**, 747-759 (2023).
- 585 20. Li, H. Fast construction of FM-index for long sequence reads. *Bioinformatics* **30**, 3274-5 (2014).
- 586 21. Wan, Y. *et al.* Systematic identification of intergenic long-noncoding RNAs in mouse retinas using full-length isoform sequencing. *BMC Genomics* **20**, 559 (2019).

608 22. Kelley, D. & Rinn, J. Transposable elements reveal a stem cell-specific class of long noncoding
609 RNAs. *Genome Biol* **13**, R107 (2012).

610 23. Johnson, R. & Guigo, R. The RIDL hypothesis: transposable elements as functional domains of
611 long noncoding RNAs. *RNA* **20**, 959-76 (2014).

612 24. Zhang, X. & Meyerson, M. Illuminating the noncoding genome in cancer. *Nat Cancer* **1**, 864-872
613 (2020).

614 25. Soneson, C. et al. A comprehensive examination of Nanopore native RNA sequencing for
615 characterization of complex transcriptomes. *Nat Commun* **10**, 3359 (2019).

616 26. Laehnemann, D., Borkhardt, A. & McHardy, A.C. Denoising DNA deep sequencing data-high-
617 throughput sequencing errors and their correction. *Brief Bioinform* **17**, 154-79 (2016).

618 27. Smith-Unna, R., Boursnell, C., Patro, R., Hibberd, J.M. & Kelly, S. TransRate: reference-free
619 quality assessment of de novo transcriptome assemblies. *Genome Res* **26**, 1134-44 (2016).

620 28. Xingyu Liao, M.L., You Zou, Fang-Xiang Wu, Yi-Pan, Jianxin Wang. Current challenges and
621 solutions of de novo assembly. *Quantitative Biology* **7**, 19 (2019).

622 29. Raghavan, V., Kraft, L., Mesny, F. & Rigerte, L. A simple guide to de novo transcriptome assembly
623 and annotation. *Brief Bioinform* **23**(2022).

624 30. Dong, X. et al. The long and the short of it: unlocking nanopore long-read RNA sequencing data
625 with short-read differential expression analysis tools. *NAR Genom Bioinform* **3**, lqab028 (2021).

626 31. Mak, Q.X.C., Wick, R.R., Holt, J.M. & Wang, J.R. Polishing De Novo Nanopore Assemblies of
627 Bacteria and Eukaryotes With FMLRC2. *Mol Biol Evol* **40**(2023).

628 32. Simão, F.A., Waterhouse, R.M., Ioannidis, P., Kriventseva, E.V. & Zdobnov, E.M. BUSCO:
629 assessing genome assembly and annotation completeness with single-copy orthologs.
Bioinformatics **31**, 3210-2 (2015).

630 33. Grabherr, M.G. et al. Full-length transcriptome assembly from RNA-Seq data without a reference
631 genome. *Nat Biotechnol* **29**, 644-52 (2011).

632 34. Mattick, J.S. et al. Long non-coding RNAs: definitions, functions, challenges and
633 recommendations. *Nat Rev Mol Cell Biol* **24**, 430-447 (2023).

634 35. Xu, X. et al. A systematic review of computational methods for predicting long noncoding RNAs.
Brief Funct Genomics **20**, 162-173 (2021).

635 36. Wucher, V. et al. FEELnc: a tool for long non-coding RNA annotation and its application to the
636 dog transcriptome. *Nucleic Acids Res* **45**, e57 (2017).

637 37. Quinlan, A.R. & Hall, I.M. BEDTools: a flexible suite of utilities for comparing genomic features.
Bioinformatics **26**, 841-2 (2010).

638 38. Stoler, N. & Nekrutenko, A. Sequencing error profiles of Illumina sequencing instruments. *NAR
639 Genom Bioinform* **3**, lqab019 (2021).

640 39. Ji, S.C.J.N.K.T.J.M.B.L.M.K.R.H.P.G.M.W.T.W.H. Overcoming High Nanopore Basecaller Error
641 Rates for DNA Storage via Basecaller-Decoder Integration and Convolutional Codes. *IEEE
642 International Conference on Acoustics, Speech and Signal Processing*, 8822-8826 (2020).

643 40. Kent, W.J. BLAT--the BLAST-like alignment tool. *Genome Res* **12**, 656-64 (2002).

644 41. Tariq, M.A., Kim, H.J., Jejelowo, O. & Pourmand, N. Whole-transcriptome RNAseq analysis from
645 minute amount of total RNA. *Nucleic Acids Res* **39**, e120 (2011).

646 42. Lopes, I., Altab, G., Raina, P. & de Magalhães, J.P. Gene Size Matters: An Analysis of Gene
647 Length in the Human Genome. *Front Genet* **12**, 559998 (2021).

648 43. Hölzer, M. & Marz, M. De novo transcriptome assembly: A comprehensive cross-species
649 comparison of short-read RNA-Seq assemblers. *Gigascience* **8**(2019).

650 44. Niazi, F. & Valadkhan, S. Computational analysis of functional long noncoding RNAs reveals lack
651 of peptide-coding capacity and parallels with 3' UTRs. *Rna* **18**, 825-43 (2012).

652 45. Wang, L. et al. CRISPR-Cas13d screens identify KILR, a breast cancer risk-associated lncRNA
653 that regulates DNA replication and repair. *Mol Cancer* **23**, 101 (2024).

654 46. NE, I.I. et al. Long non-coding RNAs and enhancer RNAs regulate the lipopolysaccharide-
655 induced inflammatory response in human monocytes. *Nat Commun* **5**, 3979 (2014).

656 47. Roux, B.T., Heward, J.A., Donnelly, L.E., Jones, S.W. & Lindsay, M.A. Catalog of Differentially
657 Expressed Long Non-Coding RNA following Activation of Human and Mouse Innate Immune
658 Response. *Front Immunol* **8**, 1038 (2017).

659 48. Khachane, A.N. & Harrison, P.M. Mining mammalian transcript data for functional long non-
660 coding RNAs. *PLoS One* **5**, e10316 (2010).

661

662

663

664 49. Frankish, A. *et al.* GENCODE reference annotation for the human and mouse genomes. *Nucleic*
665 *Acids Res* **47**, D766-d773 (2019).

666 50. Lorenzi, L. *et al.* The RNA Atlas expands the catalog of human non-coding RNAs. *Nat Biotechnol*
667 **39**, 1453-1465 (2021).

668 51. Mattick, J.S. & Rinn, J.L. Discovery and annotation of long noncoding RNAs. *Nat Struct Mol Biol*
669 **22**, 5-7 (2015).

670 52. Nurk, S. *et al.* The complete sequence of a human genome. *Science* **376**, 44-53 (2022).

671 53. Seifuddin, F. *et al.* lncRNAKB, a knowledgebase of tissue-specific functional annotation and trait
672 association of long noncoding RNA. *Sci Data* **7**, 326 (2020).

673 54. Cabili, M.N. *et al.* Integrative annotation of human large intergenic noncoding RNAs reveals global
674 properties and specific subclasses. *Genes Dev* **25**, 1915-27 (2011).

675 55. Yuan, H. *et al.* CancerSEA: a cancer single-cell state atlas. *Nucleic Acids Res* **47**, D900-d908
676 (2019).

677 56. Lanzós, A. *et al.* Discovery of Cancer Driver Long Noncoding RNAs across 1112 Tumour
678 Genomes: New Candidates and Distinguishing Features. *Sci Rep* **7**, 41544 (2017).

679 57. Bao, Z. *et al.* LncRNADisease 2.0: an updated database of long non-coding RNA-associated
680 diseases. *Nucleic Acids Res* **47**, D1034-d1037 (2019).

681 58. Petrov, A.I. *et al.* RNACentral: a comprehensive database of non-coding RNA sequences. *Nucleic*
682 *Acids Res* **45**, D128-d134 (2017).

683 59. Moradi Marjaneh, M. *et al.* Non-coding RNAs underlie genetic predisposition to breast cancer.
684 *Genome Biol* **21**, 7 (2020).

685 60. Almeida, I. GRADE2: General RNAseq Analysis for Differential Expression (version 2). Vol. 2024
686 (GitHub, 2024).

687 61. Almeida, I. GitHub repository: HyDRA pipeline. Vol. 2024 (<https://github.com/isabela42/HyDRA>,
688 2024).

689 62. Heberle, H., Meirelles, G.V., da Silva, F.R., Telles, G.P. & Minghim, R. InteractiVenn: a web-
690 based tool for the analysis of sets through Venn diagrams. *BMC Bioinformatics* **16**, 169 (2015).

691 63. De Coster, W. & Rademakers, R. NanoPack2: population-scale evaluation of long-read
692 sequencing data. *Bioinformatics* **39**(2023).

693 64. Andrews, S. FastQC.

694 65. Ewels, P., Magnusson, M., Lundin, S. & Käller, M. MultiQC: summarize analysis results for
695 multiple tools and samples in a single report. *Bioinformatics* **32**, 3047-8 (2016).

696 66. Li, H. GitHub repository: seqtk, a toolkit for processing sequences in FASTA/Q formats. Vol. 2024
697 (<https://github.com/lh3/seqtk>, 2023).

698 67. Wick, R. GitHub repository: Porechop, an adapter trimmer for Oxford Nanopore reads. Vol. 2024
699 (<https://github.com/rrwick/Porechop>, 2018).

700 68. Martin, M. Cutadapt Removes Adapter Sequences From High-Throughput Sequencing Reads.
701 *EMBnet.journal* **17**, 10-12 (2011).

702 69. Song, L. & Florea, L. Rcorrector: efficient and accurate error correction for Illumina RNA-seq
703 reads. *Gigascience* **4**, 48 (2015).

704 70. Bushnell, B. BBMap: A short read aligner. Vol. 2024 (SourceForge, 2023).

705 71. Freedman, A.H. GitHub repository: Transcriptome Assembly Tools, a collection of scripts for
706 processing fastq files in ways to improve de novo transcriptome assemblies, and for evaluating
707 those assemblies. Vol. 2024
708 (<https://github.com/harvardinformatics/TranscriptomeAssemblyTools>, 2023).

709 72. Bolger, A.M., Lohse, M. & Usadel, B. Trimmomatic: a flexible trimmer for Illumina sequence data.
710 *Bioinformatics* **30**, 2114-20 (2014).

711 73. Langmead, B. & Salzberg, S.L. Fast gapped-read alignment with Bowtie 2. *Nat Methods* **9**, 357-
712 9 (2012).

713 74. Danecek, P. *et al.* Twelve years of SAMtools and BCFtools. *Gigascience* **10**(2021).

714 75. Wang, L., Wang, S. & Li, W. RSeQC: quality control of RNA-seq experiments. *Bioinformatics* **28**,
715 2184-5 (2012).

716 76. Ramírez, F. *et al.* deepTools2: a next generation web server for deep-sequencing data analysis.
717 *Nucleic Acids Res* **44**, W160-5 (2016).

718 77. Camacho, C. *et al.* BLAST+: architecture and applications. *BMC Bioinformatics* **10**, 421 (2009).

719 78. Edwards, J.A.E.R.A. Fastq-pair: efficient synchronization of paired-end fastq files. *bioRxiv preprint*(2019).

720 79. Wu, T.D. & Watanabe, C.K. GMAP: a genomic mapping and alignment program for mRNA and EST sequences. *Bioinformatics* **21**, 1859-75 (2005).

721 80. Bergelson, L. Picard: A set of command line tools (in Java) for manipulating high-throughput sequencing (HTS) data and formats such as SAM/BAM/CRAM and VCF. Vol. 2024 (GitHub, 2023).

722 81. Li, H. Minimap2: pairwise alignment for nucleotide sequences. *Bioinformatics* **34**, 3094-3100 (2018).

723 82. Fu, L., Niu, B., Zhu, Z., Wu, S. & Li, W. CD-HIT: accelerated for clustering the next-generation sequencing data. *Bioinformatics* **28**, 3150-2 (2012).

724 83. Neph, S. *et al.* BEDOPS: high-performance genomic feature operations. *Bioinformatics* **28**, 1919-20 (2012).

725 84. Nullmodel), U.H. GitHub repository: kentUtils, UCSC command line bioinformatic utilities. Vol. 2024 (<https://github.com/ENCODE-DCC/kentUtils>, 2014).

726 85. Bonfield, J.K. *et al.* HTSlib: C library for reading/writing high-throughput sequencing data. *Gigascience* **10**(2021).

727 86. Moore, B. GitHub repository: Genome Annotation Library, a perl toolkit for working with SO compliant genome annotations. Vol. 2024 (<https://github.com/The-Sequence-Ontology/GAL>, 2012).

728 87. Wang, M. & Kong, L. pblast: a multithread blat algorithm speeding up aligning sequences to genomes. *BMC Bioinformatics* **20**, 28 (2019).

729

730

731

732

733

734

735

736

737

738

739

740

741